2016 24th International Lightning Detection Conference
18 - 19 April | San Diego, California, USA
6th International Lightning Meteorology Conference
20 - 21 April | San Diego, California, USA

Relationship between the average number of sensors reporting and the detection efficiency of a network

Wolfgang Schulz
ALDIS
OVE Service GmbH
Vienna, Austria

Amitabh Nag, Martin J. Murphy
Vaisala Inc.,
Louisville, CO, U.S.A.

***Abstract*—In this paper we want to shed some light on the relation between the DE and the average number of sensors reporting (ANSR). For this purpose we use a simple detection efficiency (DE) model. We validate the simple DE model with real data from the EUCLID network and show that even with such a simple model the agreement between the modeled and the observed ANSR is reasonable. We further show that observed ANSR cannot be used to estimate the DE for networks containing only a few sensors and networks with large sensor baselines. In such networks, more advanced analysis and modeling of the full NSR distribution is necessary. In general, we suggest that the probability of DE given a certain ANSR is a more reasonable way to describe the ANSR-DE relationship.**

Keywords—lightning; lightning location systems; performance analysis, network self-reference

I. INTRODUCTION

The network self-reference technique is a method to validate the performance characteristics of a lightning locating system (LLS) that involves statistical analysis of parameters reported by the LLS itself, such as standard deviation of sensor timing error, semi major axis length of the 50% confidence ellipse, and the number of sensors reporting (NSR), to infer its location accuracy (LA) and detection efficiency (DE) [*Nag et al.*, 2015].

The method of deriving the LA of a LLS in a particular region by using the median semi major axis length of the confidence ellipses for cloud-to-ground strokes geolocated by the LLS in that region is well understood. Note that the confidence ellipse is accurate as long as the standard deviations of the time and angle measurements for each sensor are represented properly and bias errors have been corrected [*Diendorfer et al.*, 2014].

As first described by [*Cummins et al.*, 1992], there exists a relationship between the average number of sensors reporting (ANSR) and the DE of an LLS. In this paper, we extend the original concept of an ANSR model by representing each sensor's DE in the space of the sensor's dynamic range. Simultaneously, we also simplify certain aspects of the model in order to demonstrate both the capabilities and limitations of comparing a simple model of ANSR with observations of ANSR from an operational LLS. Specifically, using data from the EUCLID network, we show that a reasonable match is obtained between the model-predicted ANSR of negative CG strokes and the actual ANSR reported by the network. We also explore the relationship between ANSR and negative CG stroke DE for different sensor baselines and network sizes (total number of sensors).

II. THE MODEL

We consider a generic sensor type rather than any specific one. Each sensor in the network is assumed to have an 80% chance of detecting a lightning event (cloud-to-ground stroke or cloud pulse) as long as the radiated peak field of the event at the sensor location crosses the detection threshold of the sensor. If the peak field of the event is below the sensor's detection threshold, the probability of detection by that sensor is assumed to be zero. We ignore any saturation effect at the sensor.

By decoupling the sensor DE curve from direct convolution with either distance or a specific peak current distribution, we are able to model a distribution of NSR values at any arbitrary value of peak current, independent of lightning type. Then, we can produce a weighted average of NSR that is based on any distribution of peak current (or equivalent peak current), so that we can produce curves of modeled ANSR versus DE that are specific to negative cloud-to-ground (CG) strokes, positive CG strokes, or different types of cloud discharges, as needed.

To estimate the radiated E-field at any sensor position we take into account the field attenuation along the propagation path using the attenuation model from [*CIGRE Report 376*, 2010] and [*Diendorfer et al.*, 2009], which has an e-folding length λ=1000 km,.

For the DE and ANSR simulations related to network size and sensor baseline the sensor gain is assumed to be 4 for all the sensors. Further the thresholds are assumed to be 0.37 V/m for all sensors in simulated networks. For the DE and ANSR evaluations of the EUCLID network, the individual sensor gains and thresholds of the actual sensors are used.

For the model based estimation of the ANSR, the coverage area of the network is divided in regular grid cells. In each grid cell, for each peak current of a log-normal peak current distribution (I_{median} = 12 kA, σ_{ln} = 0.6) representative of negative subsequent CG strokes, the algorithm of the model checks if the radiated signal crosses the threshold at the distance of each sensor of the network. It then calculates the probability that the stroke is detected by each combination of sensors that could yield a geo-location, as described in equation B1 of [*Nag et al.*, 2015]. In the interest of simplifying to the case of a sufficiently large network, however, we do not explicitly remove sensor combinations that result in large random location errors, as indicated by [*Nag et al.*, 2015], nor do we impose a maximum distance limit as is often done operationally. Finally, at each grid cell, the probability-weighted average of the NSR values of all possible sensor combinations yields the ANSR.

Flash-DE is calculated according to [*Rubinstein*, 1995] with the assumption that the stroke DE is independent of stroke order. We use a multiplicity distribution determined from the video and E-field measurements in Austria [*Schulz et al.*, 2010], [*Schulz et al.*, 2012]. The average multiplicity of those flashes was 3.42.

In order to check the validity of the model for the EUCLID network, the model was tested over narrow ranges of amplitudes to avoid the influence of the specific shape of the peak current distribution. The resulting model-calculated ANSR for a peak current of -12 kA is shown in Fig. 1. For comparison, Fig. 2 shows the real ANSR in the EUCLID network over the years 2010-2014 and a peak current range of -11 kA to -13 kA. The differences between the modeled ANSR and the real ANSR in some regions of the network are caused by the following reasons:

- The model uses a general attenuation model for the entire network and thus ignores local ground conductivity changes. This is particularly important in the Alpine region, where the model overestimates ANSR, but in other areas, the assumption of a single, uniform attenuation model leads the same model to underestimate ANSR.
- The model necessarily must assume ideal communication between the sensors and the central processor, which obviously is not always true in an operational LLS.
- Although sensor thresholds and gains were changed for several sensors during those years, we use the latest configuration values in the calculations. These differences can lead to over- or underestimation, depending on the details of the specific changes.

Nevertheless the agreement between model and the real ANSR is surprisingly good. We also compared the modeled ANSR with the real ANSR for a peak current of –25 kA with similar results (not shown here).

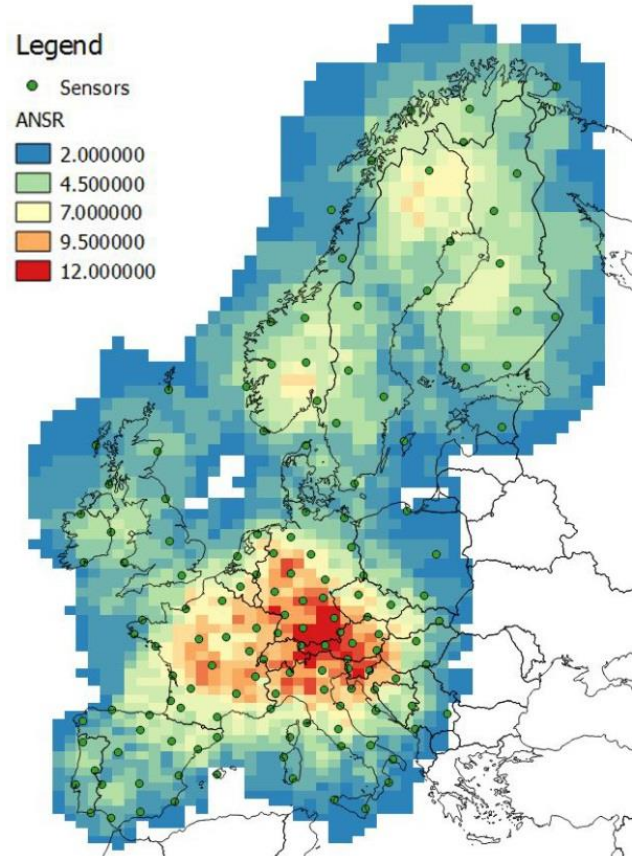

Fig. 1. Model calculated ANSR for a peak current of -12 kA.

III. ANSR FOR DIFFERENT NETWORK CONFIGURATIONS

In this section, we want to investigate the general relationship between stroke DE and ANSR. To test this relationship, we calculated both quantities for different network sizes and different sensor baselines. Fig. 3 shows the spatial patterns of DE (upper figures) and ANSR (lower figures) for three different networks with 100 km sensor baselines, a 4 (A), a 9 (B), and a 16 (C) sensor network.

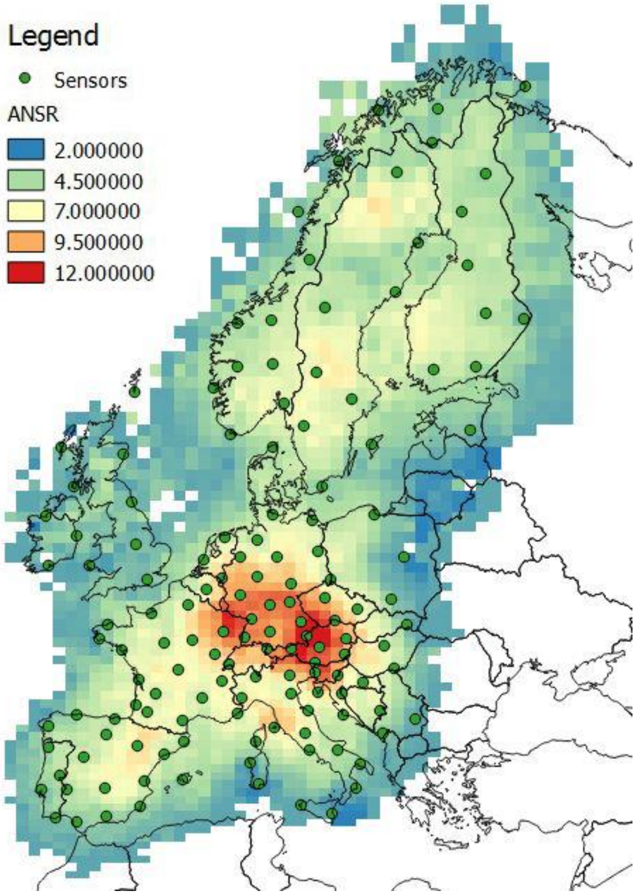

Fig. 2. ANSR from EUCLID data 2010-2014 for -11 kA to -13 kA.

The relationship between stroke DE and ANSR for a network with 100 km sensor baseline is shown in Fig. 4A. It contains the relation between ANSR and stroke DE for networks with 4 sensors (green "+"), 9 sensors (red "+") and 16 sensors (blue "+"). Each "+" represents an individual grid cell. Fig. 4B and Fig. 4C show the similar simulation for networks with 200 and 300 km sensor baseline, respectively. Fig. 4 indicates that the relationship between ANSR and stroke DE strongly depends on the sensor baseline and the number of sensors in the network. These simulations further show that

- for networks with a small number of sensors (< 9), there is no dependence between DE and ANSR given the simple model that we have implemented in this work.
- the larger the baseline, the lower the overall ANSR and the smaller the dependence of DE on ANSR.

Therefore, the interpretation of ANSR observations with the aid of a simplified model is only useful in networks containing at least 9 sensors and where the baselines are shorter than about 200 km. To address small networks or networks with much longer sensor baselines, a complete model of the NSR distribution as a function of peak current is needed. That model also must include the effects of sensor saturation and the coupling between location accuracy and detection efficiency, as described in Appendix B of [*Nag et al.*, 2015] .

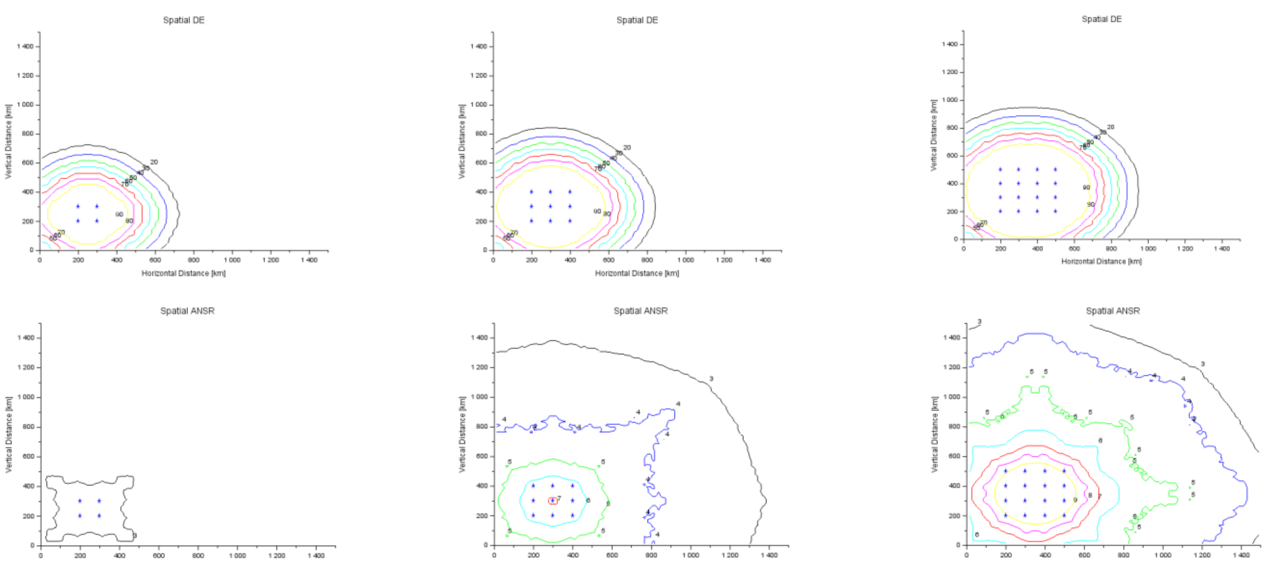

A) B) C)

Fig. 3. Three different network configurations for a 100 km baseline with A) 4 sensors, B) 9 sensors and C) 16 sensors. Blue stars are the assumed sensor locations.Upper figures show the spatial stroke DE and the lower figures the correspong ANSR.

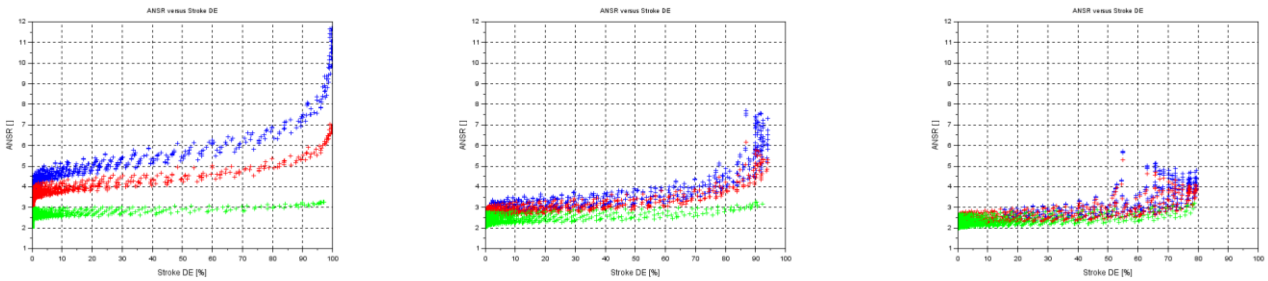

A) B) C)

Fig. 4. Stroke DE versus ANSR for different network configurations. A) 100 km sensor baseline. B) 200 km sensor baseline. C) 300km sensor baseline. Each figure contains three network sizes, green “+” 4 sensor network, red “+”9 sensor network, blue “+”16 sensor network.

IV. ANSR – DE RELATIONSHIP FOR THE EUCLID NETWORK

We also use the model described above to estimate the relationship between ANSR and DE for strokes and flashes for the EUCLID network.

In Fig. 5 we present the observed ANSR for all negative subsequent strokes of the EUCLID network. We use negative subsequent strokes because their peak current distribution is similar to what we assumed in the model. The modeled ANSR is given in Fig. 6. The most obvious difference between the two is the representation by the model of ANSR far outside the network. The difference is due to the fact that our simple model ignores both a maximum distance limit and a maximum ellipse size, which are both present in the real location algorithm. As already mentioned in section II, the model can either over- or underestimate the ANSR in various regions of the network depending on the particular signal propagation conditions and sensor configurations. Especially in the Alps, a region of low ground conductivity, ANSR is overestimated by the model due to the absence of a propagation attenuation model specific to that region. Nevertheless the general agreement between the model output and the real data is surprisingly good for such a simple model.

Fig. 7 shows the spatial distribution of stroke DE of the EUCLID network. Again, it is important to keep in mind that the model ignores any maximum distance and maximum ellipse criteria, and therefore, DE is overestimated in regions far away from the network.

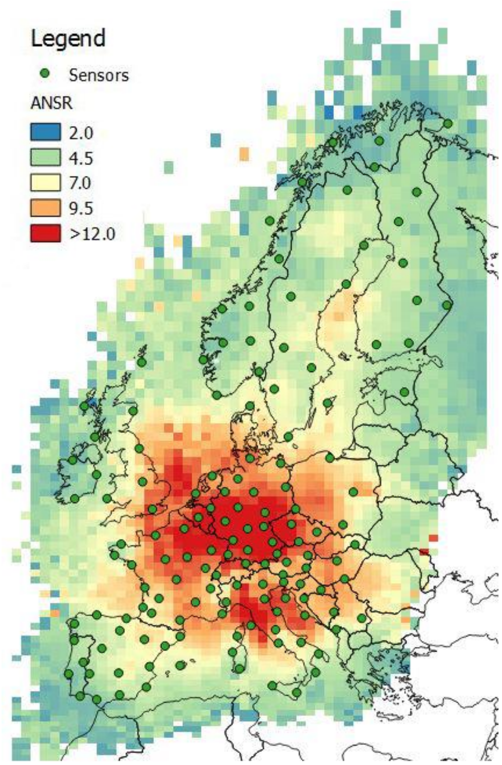

Fig. 5. ANSR for all negative subsequent strokes from the EUCLID network during the period 2010-2014.

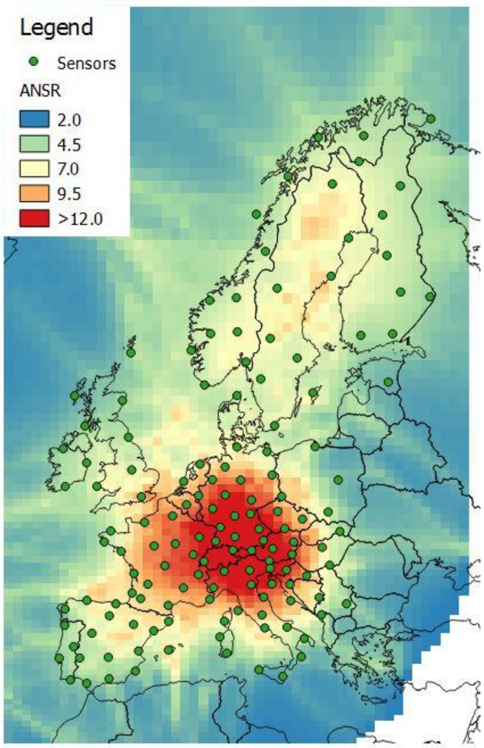

Fig. 6. ANSR from the DE model for all negative strokes for the EUCLID network.

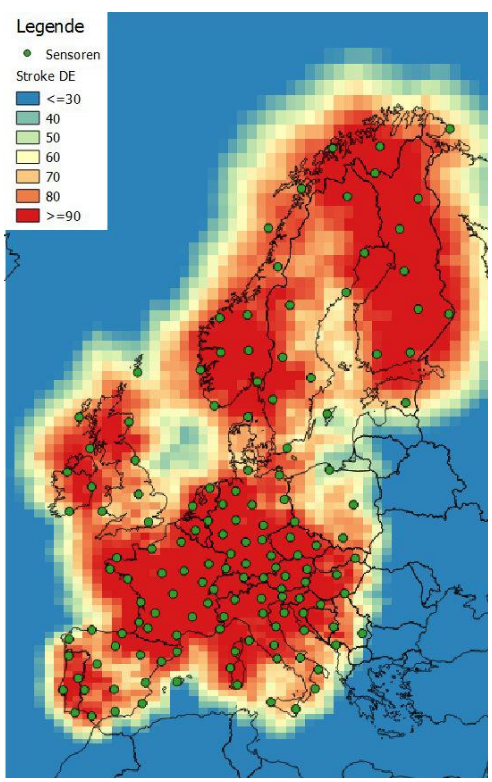

Fig. 7. Modeled stroke DE of the EUCLID network

The relationship between ANSR and stroke DE for the EUCLID network is given in Fig. 8 (green +). The flash DE is calculated from the stroke DE according to [*Rubinstein*, 1995] as mentioned in section II and also shown in Fig. 8 (red "+"). The general relation between the ANSR and the stroke/flash DE seen in Fig. 8 is similar to what is shown for different network configurations in Fig. 4. The transfer of stroke DE to flash DE generally moves the DE towards larger values, which makes it more complicated to assess flash DE using ANSR observations coupled with a simple model. It is also important to note that the flash DE values shown in Fig. 8 are somewhat limited because they are inferred from stroke DE based on a subsequent stroke peak current distribution and from a particular distribution of multiplicity values.

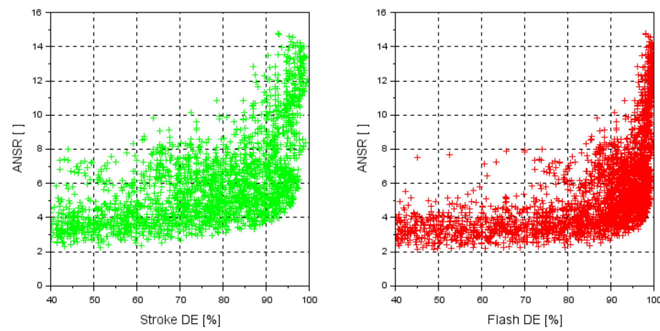

Fig. 8. ANSR versus stroke DE (green +) and flash DE (red +)

Given the relationship between ANSR and DE shown in Figures 4 and 8, we assert that it is not generally useful to infer a single DE value from an observed value of ANSR because the two do not have a linear relationship. Instead, a given ANSR represents a range of DE values with a particular probability distribution. Fig. 9 shows this probabilistic interpretation of the same data shown in Fig. 8, in other words, the probability of particular stroke DE ranges given different ANSRs.

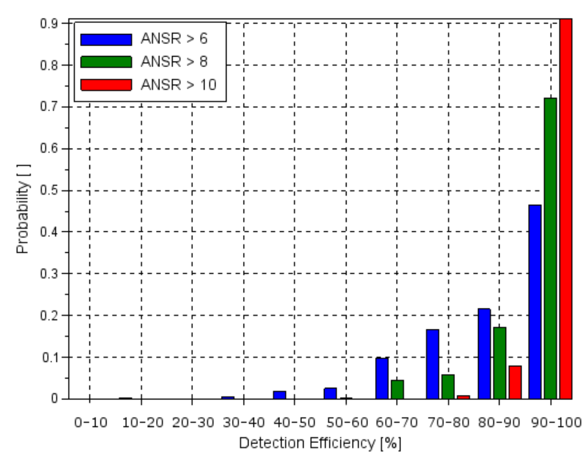

Fig. 9. Probability of stroke DEs for certain ANSRs

In Fig. 9 we see that there is a 90% probability that an ANSR greater than 10 corresponds to a stroke DE above 90%

and a ~72% probability that an ANSR above 8 corresponds to a stroke DE above 90%.

The resulting modeled flash DE for the EUCLID network is given in Fig. 10. As mentioned above, the simulation is performed with a peak current distribution for subsequent strokes and a particular multiplicity distribution. Because negative first strokes, as well as positive strokes, exhibit larger peak currents on average than subsequent strokes, the simulation in Fig. 10 is assumed to be a lower limit on the flash DE. Validation studies [*Schulz et al.*, 2014] show that the resulting output of the model is reasonable.

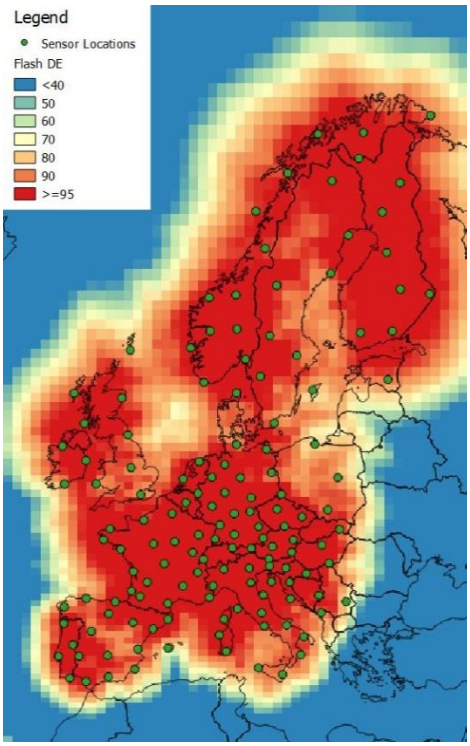

Fig. 10. Modeled flash DE based on a peak current distribution for negative subsequent strokes

V. SUMMARY

DE models are often used to predict the performance of an LLS. A byproduct of such DE models is the ANSR, which is sometimes used to evaluate the performance of an operational LLS because ANSR is observed directly in the LLS data. We showed in this paper that even with a very simple DE / ANSR model, model estimates of ANSR can agree reasonably well with observations. However, simulations with different network sizes and different sensor baselines show that there is no dependence between the modeled ANSR and DE in small networks (< ~9 sensors) or in networks with baselines greater than about 200 km. Therefore, to make use of observed NSR from such networks in self-reference studies, it is necessary to move to a more advanced analysis of the full two-dimensional distribution of NSR as a function of peak current. The model employed in such studies must also include the various effects that were ignored in this paper, such as sensor saturation, the maximum size of the error ellipse allowed in operation, as well as any maximum distance limit.

In networks with more sensors and shorter baselines, the simplifying assumptions used in this study are generally valid. Even so, the relation between DE and ANSR is not straightforward. Therefore, we suggest interpreting ANSR values in terms of the corresponding probability that stroke DE is at or above a certain level (see Fig. 9).

ACKNOWLEDGMENT

We want to thank Gerhard Diendorfer for his helpful comments.

REFERENCES

CIGRE Report 376 (2010), *Cloud-to-Ground Lightning Parameters Derived from Lightning Location Systems - The Effects of System Performance*, CIGRE Report 376.

Cummins, K. L., W. L. Hiscox, A. E. Pifer, and M. W. Maier (1992), Performance Analysis of the U.S. National Lightning Detection Network, in *International Conference on Atmospheric Electricity (ICAE)*.

Diendorfer, G. et al. (2009), Review of CIGRE Report "Cloud-to-Ground Lightning Parameters Derived from Lightning Location Systems – The Effects of System Performance," in *CIGRE*.

Diendorfer, G., H. Pichler, and W. Schulz (2014), EUCLID Located Strokes to the Gaisberg Tower – Accuracy of Location and its assigned Confidence Ellipse, in *International Lightning Detection Conference and International Lightning Meteorology Conference (ILDC/ILMC)*, Tucson.

Nag, A., M. J. Murphy, W. Schulz, and K. L. Cummins (2015), Lightning Locating Systems: Insights on Characteristics and Validation Techniques, *Earth Sp. Sci.*, (2), 65–93, doi:10.1002/2014EA000051.

Rubinstein, M. (1995), On the Determination of the Flash Detection Efficiency of Lightning Location Systems given their Stroke Detection Efficiency, in *International Symposium on Electromagnetic Compatibility (EMC)*, pp. 429–432.

Schulz, W., H. Pichler, and G. Diendorfer (2010), Evaluation of 45 negative flashes with e-field measurements, video data and lightning location data in Austria, in *Lightning Protection (ICLP), 2010 International Conference on*, pp. 7–10, Cagliari, Italy.

Schulz, W., C. Vergeiner, H. Pichler, G. Diendorfer, and S. Pack (2012), Validation of the Austrian Lightning Location System ALDIS for negative Flashes, in *CIGRE C4 Colloquium on Power Quality and Lightning*, pp. 13–16.

Schulz, W., D. R. Poelman, S. Pedeboy, C. Vergeiner, H. Pichler, G. Diendorfer, and S. Pack (2014), Performance Validation of the European Lightning Location System EUCLID, in *CIGRE International Colloquium on Lightning and Power systems*.